

Transition to superfluid turbulence governed by an intrinsic parameter

A.P. Finne^{*}, T. Araki[§], R. Blaauwgeers^{*,†},
V.B. Eltsov^{*,‡}, N.B. Kopnin^{*,||}, M. Krusius^{*},
L. Skrbek¹, M. Tsubota[§], & G.E. Volovik^{*,||}

^{*} *Low Temperature Laboratory, Helsinki University of Technology, P.O.Box 2200, FIN-02015 HUT, Finland.*

[§] *Department of Physics, Osaka City University, Sumiyoshi-Ku, Osaka 558-8585, Japan.*

[†] *Kamerlingh Onnes Laboratory, Leiden University, P.O.Box 9504, 2300 RA Leiden, The Netherlands.*

[‡] *Kapitza Institute for Physical Problems, Kosygina 2, 119334 Moscow, Russia.*

^{||} *Landau Institute for Theoretical Physics, Kosygina 2, 119334 Moscow, Russia.*

¹ *Joint Low Temperature Laboratory, Institute of Physics ASCR and Charles University, Prague, Czech Republic.*

Hydrodynamic flow in both classical and quantum fluids can be either laminar or turbulent. To describe the latter, vortices in turbulent flow are modelled with stable vortex filaments. While this is an idealization in classical fluids, vortices are real topologically stable quantized objects in superfluids. Thus superfluid turbulence [1] is thought to hold the key to new understanding on turbulence in general. The fermion superfluid ^3He offers further possibilities owing to a large variation in its hydrodynamic characteristics over the experimentally accessible temperatures. While studying the hydrodynamics of the B phase of superfluid ^3He , we discovered a sharp transition at $0.60 T_c$ between two regimes, with regular behaviour at high-temperatures and turbulence at low-temperatures. Unlike in classical fluids, this transition is insensitive to velocity and occurs at a temperature where the dissipative vortex damping drops below a critical limit. This discovery resolves the conflict between existing high- and low-temperature measurements in $^3\text{He-B}$: At high temperatures in rotating flow a vortex loop injected into superflow has been observed to expand monotonically to a single rectilinear vortex line [2–4], while at very low temperatures a tangled network of quantized vortex lines can be generated in a quiescent bath with a vibrating wire [5]. The solution of this conflict reveals a new intrinsic criterion for the existence of superfluid turbulence.

In conventional liquids the vorticity $\boldsymbol{\omega} = \nabla \times \mathbf{v}$ obeys the Navier-Stokes equation

$$\frac{\partial \boldsymbol{\omega}}{\partial t} = \nabla \times [\mathbf{v} \times \boldsymbol{\omega}] + \nu \nabla^2 \boldsymbol{\omega}.$$

The interplay of the two terms on the rhs, the inertial first term and the viscous second term, governs the transition to turbulence [6]. It is determined by the external

conditions through the Reynolds number, $Re = RU/\nu$, formed by the characteristic size R of the system, the flow velocity U , and the kinematic viscosity ν . At large $Re \gg 1$, the effect of the inertial term is dominating, and laminar flow becomes increasingly unstable. If vorticity is released into a meta-stable laminar state, a sudden transition to a chaotic flow of eddies occurs. The evolution of the turbulent flow is described by the Kolmogorov energy cascade: the kinetic energy of the flow is transferred to ever smaller length scales, with large vortex loops decaying into smaller loops, until a scale is reached where the energy is dissipated by viscosity.

In superfluids turbulence acquires new features: A superfluid can be described as consisting of two interpenetrating fractions, the frictionless (superfluid) and viscous (normal) components. If both fractions are moving, as is the case *eg.* behind a pulled grid in measurements on superfluid turbulence in ^4He [1], the turbulent state bears more resemblance to that of viscous liquids. A new class of superfluid turbulence becomes possible when the normal component is so viscous that it is essentially immobile and only the superfluid component is moving with respect to the boundaries. This is the usual case in the flow of ^3He , which is considered here.

The vorticity of the superfluid component is quantized in terms of the circulation quantum $\kappa = 2\pi\hbar/M$ where M is the mass of a superfluid particle. The flow of the superfluid component can be characterized with the ‘superfluid Reynolds number’ $Re_s = RU/\kappa$. The Feynman criterion $Re_s \sim 1$ gives the velocity at which it becomes energetically favorable to form a quantized vortex. If a large nucleation barrier exists, vortices are not created and the superfluid remains vortex-free, in our measurements here up to $Re_s \sim 200$. Quantized vortices can then be injected, either by some extrinsic means or by increasing the velocity so that the nucleation barrier is overcome and spontaneous vortex formation occurs. The limit of large $Re_s \gg 1$ is equivalent to a vanishing Planck’s constant, $\kappa \propto \hbar \rightarrow 0$, so that the vorticity becomes a continuous variable, like in the classical case. However, the fluid still remains unconventional because of its two-fluid nature: In addition to the superflow, there is the normal component which is at rest in the container frame, $\mathbf{v}_n = 0$. Interactions between the superfluid vorticity and the normal component give rise to a mutual friction force on a unit volume of the superfluid,

$$\mathbf{f}_{\text{mf}} = -\alpha' \rho_s [\mathbf{v}_s \times \boldsymbol{\omega}_s] + \alpha \rho_s [\hat{\boldsymbol{\omega}}_s \times [\boldsymbol{\omega}_s \times \mathbf{v}_s]],$$

which is described by the dimensionless temperature-dependent parameters α and α' . These correspond to the usual mutual friction parameters, if we are dealing with one vortex or locally polarized vorticity, or they may be renormalized in the general case. Here \mathbf{v}_s and $\boldsymbol{\omega}_s = \nabla \times \mathbf{v}_s$ are the superfluid velocity and vorticity, and $\hat{\boldsymbol{\omega}}_s$ is the unit vector in the direction of $\boldsymbol{\omega}_s$. Inserting the mutual-friction force in the Euler equation one obtains the hydrodynamic equation for $Re_s \gg 1$ [7]:

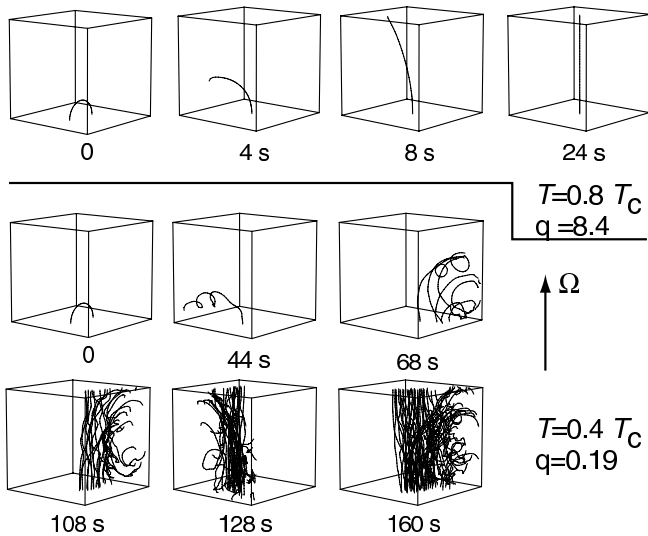


FIG. 1. Summary of events: A vortex half ring is injected into *vortex-free* superflow, generated with rotation around the vertical axis ($\Omega = 0.21$ rad/s or $\text{Re}_s \approx 30$). The figures represent snapshots from simulation calculations in the rotating frame, which are consistent with the experimental observations. The only temperature dependence is contained in the mutual-friction parameters α and α' which we take from Ref. [10]. (*Top*) At high temperatures the loop grows monotonically into a single rectilinear vortex line, pulled by the Magnus force from the superflow. The motion is highly damped since the Magnus force is balanced by the mutual friction force. (*Bottom*) At low temperatures the loop moves with the circulating superflow: (44 s) The vortex is unstable with respect to loop formation and develops through reconnections into a tangle at the injection site. (68 s) The Magnus force from the vortex-free superflow extends the tangle along the vertical axis. The measured flight time τ_F for the tangle to extend across a vertical distance d is controlled by mutual-friction damping: $\tau_F \approx d/(\Omega R \alpha)$. (108 — 160 s) The final step is the reconnection of the tangle to rectilinear lines. The growth in the relative polarization is experimentally observed as a relaxation in the NMR absorption and the total number of vortex lines in the final stable state is determined from the NMR line shape (Fig. 2).

$$\frac{\partial \omega_s}{\partial t} = (1 - \alpha') \nabla \times [\mathbf{v}_s \times \omega_s] + \alpha \nabla \times [\hat{\omega}_s \times (\omega_s \times \mathbf{v}_s)]. \quad (1)$$

The energy dissipation is determined by the mutual friction damping α in the second term, while the reactive mutual-friction α' renormalizes the inertial term of conventional hydrodynamics. Like in a classical fluid, the inertial term drives the instability by increasing the number of vortex loops, whereas the dissipative term acts to stabilize laminar flow by decreasing the number of loops. The fundamental difference from conventional hydrodynamics is that these two competing terms now have a similar dependence on the velocity and its gradients. Their

relative importance is determined by the intrinsic dimensionless parameter of the superfluid, $q = \alpha/(1 - \alpha')$, in contrast to classical liquids where it is governed via the Reynolds number by the extrinsic quantities R and U . We thus expect laminar flow to become unstable when q drops below a critical value $q_c \sim 1$. In the case of a single vortex line the parameter q also marks the crossover from propagating Kelvin waves ($q \lesssim 1$) to the over-damped regime ($q \gtrsim 1$) [8]. In Fermi superfluids and superconductors with finite energy gap one has $q \approx (\omega_0 \tau)^{-1}$, where ω_0 is the spacing between the bound states of quasiparticles in the vortex core and τ^{-1} is their lifetime broadening, owing to scattering from the normal component [9]. In $^3\text{He-B}$, q approaches infinity at T_c and drops monotonically to zero, when cooled down to $T \rightarrow 0$ [9,10]. Such an evolution of q with temperature would in classical fluids correspond to scanning the Reynolds number from 0 to ∞ : We can thus study the emergence of turbulence as a function of temperature when q falls below unity.

Measurements:—In rotating $^3\text{He-B}$ high-velocity vortex-free superflow can be achieved, into which vortex seed loops can be injected (Fig. 1). We record as a function of temperature T and rotation Ω the number of rectilinear vortex lines after injection (N_f), when all transients have died out. Non-invasive NMR measurement is used to determine the number of vortex lines in the final state. The NMR absorption spectrum of $^3\text{He-B}$ maps the order-parameter texture, which is strongly affected by the orienting effect from the \mathbf{v}_s field. It allows us to determine N_f with a resolution better than 10 vortex lines in the temperature range of Fig. 2. In Fig. 2d we list the result after each injection event in the (Ω, T) plane, classified as a regular high-temperature (*blue*) or turbulent low-temperature (*red*) process. Here the injection method is the shear-flow instability of the phase boundary between the $^3\text{He-A}$ and $^3\text{He-B}$ phases, which produces a small random number ($\Delta N \sim 10$) of B-phase vortex loops whose one end sticks out of the AB interface while the other end is on the cylindrical sample boundary [4]. At high temperatures an injected loop expands and becomes a single rectilinear vortex line. At low temperatures the loop evolves into tangled vorticity which finally fills the whole sample volume with rectilinear lines. The central plot Fig. 2d leads to a surprising conclusion: Only a narrow cross-over region at $0.60 T_c$ separates the two processes, with little dependence on the maximum superflow velocity $U = \Omega R$ of the initial vortex-free state. At the transition temperature $0.60 T_c$, the experimental value of $q = \alpha/(1 - \alpha') \approx 1.3$ [10].

Vortices can also be injected with other methods. In the absence of the AB interface vortices are created (i) at a rough spot on the cylindrical sample boundary [2], (ii) under neutron irradiation [3], or (iii) by a sudden leak of vortex loops through the small orifice which connects the sample to the rest of the liquid ^3He volume [11]. These three processes have different critical velocities and temperature dependences, but in all cases the measurements are consistent with a crossover at $0.60 T_c$ from a low-yield

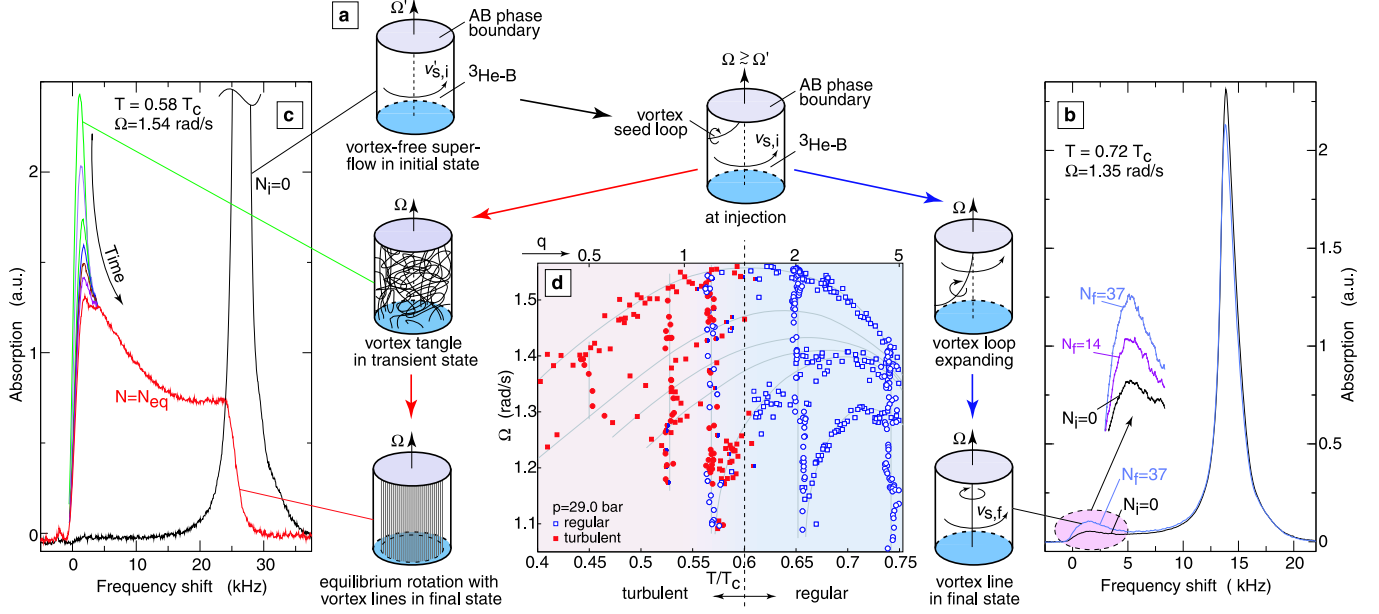


FIG. 2. Principle of measurement and central result: **a**, The initial state is vortex-free superflow in rotation, with the normal component stationary and the superfluid component moving in the rotating frame. This state is identified by a large sharp peak in the NMR absorption spectrum, which is caused by the vortex-free superflow and is shifted far from the Larmor value (line shape denoted as $N_i = 0$ in **b** and **c**). When a few (ΔN) vortex loops are injected, the number of vortex lines in the final steady state (N_f) is found to fall in one of two categories: **b**, $N_f = \Delta N$, indicated by a small shift of the NMR absorption from the superflow peak close to the Larmor value. The shifted absorption is proportional to N_f , as shown in the insert by the build up of absorption at small frequency shift. This process corresponds to regular loop expansion. **c**, $\Delta N \ll N_f \lesssim N_{eq}$, indicated by a total removal of the superflow peak (red). Here $N_{eq} \approx \pi R^2 2\Omega/\kappa \sim 10^3$ is the equilibrium number of vortex lines in rotation. This process corresponds to turbulent loop expansion. The relaxation of the line shape through intermediate stages (**c**) represents a direct signal from the turbulent epoch: In the final state with a large number of rectilinear vortex lines ($N_f \approx N_{eq}$), the distribution of absorption is relatively flat. In contrast, in the turbulent state with unpolarized \mathbf{v}_s field, much of the absorption is piled in a narrow peak at the Larmor edge. The intermediate curves between these two limiting line shapes represent the transient relaxation when the turbulent vorticity with $\omega_s \gg \omega_{eq}$ decays to a polarized cluster of rectilinear lines with $\omega_{eq} = 2\Omega$. **d**, Phase diagramme of measured events: Each data point monitors the outcome from an injection event which is initiated using the shear-flow instability of the phase boundary between $^3\text{He-A}$ and $^3\text{He-B}$. Vortex loop expansion separates into regular events (blue) and turbulent events (red) as a function of rotation Ω and temperature T , with an abrupt transition at $0.60 T_c$ independently of Ω . Only within a very narrow interval $\Delta T \sim 0.05 T_c$ around $0.60 T_c$ can intermediate values of N_f be measured. By scanning the temperature (curved lines) or the current in the magnet for stabilizing the AB phase boundary (vertical lines), the critical velocity $v_c \approx \Omega R$ of the interface instability can be varied along well-defined continuous trajectories.

to a high-yield process with decreasing temperature. Depending on sample geometry, below $0.50 T_c$ the vortex leak through the orifice may occur at 0.5 rad/s or less. Even at these low velocities ($Re_s \lesssim 70$) vortex loop expansion is found to be turbulent.

The long cylindrical sample is monitored with two signal coils at different locations, connected to independently operated NMR spectrometers. In addition to the number of vortex lines in the final stable state, we can obtain information on the transient state: (i) on the axial expansion of the vorticity and (ii) below $0.60 T_c$ on the decay of the tangle into a polarized array of rectilinear lines. The former process, the expansion of the vorticity along the $\hat{\Omega}$ axis between the two signal coils, is con-

trolled by the mutual-friction damping α : The extracted flight time for the motion in the axial direction reproduces $\alpha(T)$ from Ref. [10] and is continuous across the transition at $0.60 T_c$. Thus the axial expansion is indifferent to whether the vorticity moves as noninteracting loops or as a network of loops.

Below $0.60 T_c$, the arrival of the tangled vorticity within a pick-up coil is signalled by a massive abrupt shift of the absorption close to the Larmor edge, where a new sharp absorption peak is formed (Fig. 2c). This line shape is similar to that measured in the non-rotating state ($\Omega = 0$). Here the orientational effects from the superflow fields trapped around the vortex cores are averaged out, owing to the randomly distributed vortex tan-

gle with density $\omega_s \gg \omega_{\text{eq}}$ and the removal of essentially all large-scale vortex-free superflow. The sharp peak then decays with a relaxation time $\sim 30\text{s}$ towards the broad final stable state spectrum of a polarized vortex array with rectilinear lines and $\omega_s = \omega_{\text{eq}} = 2\Omega$. This restructuring of the NMR line shape is thus a direct signal from the transient epoch with a vortex tangle.

Numerical simulation—As seen in Fig. 1, the measured features are consistent with our simulation calculations. We use the vortex filament model [12] in the rotating frame [13]. A vortex is represented in parametric form by $\mathbf{s} = \mathbf{s}(\xi, t)$, where \mathbf{s} refers to a point on the filament and ξ is the arc length along it. The spatial and time evolutions are integrated rigorously using the Biot-Savart law. The vortex velocity $\dot{\mathbf{s}}$ is calculated from the dynamic equation $\dot{\mathbf{s}} = \mathbf{v}_{\text{sl}} + \alpha' \mathbf{s}' \times [\mathbf{s}' \times \mathbf{v}_{\text{sl}}] - \alpha [\mathbf{s}' \times \mathbf{v}_{\text{sl}}]$ (recall that $\mathbf{v}_{\text{n}} = 0$), where the local superfluid velocity \mathbf{v}_{sl} includes all contributions to the superflow at $\mathbf{s}(\xi, t)$. As boundary conditions we use smooth solid-walls with image vortices.

The initial state is a vortex half ring (diameter 3.5 mm) in the centre of a cubic sample container (10 mm wide). At high temperatures $T/T_c = 0.8$ the high damping α causes the seed loop to expand, mostly by motion in the radial and axial directions, into a single rectilinear vortex line in the centre of the sample. At low temperatures $T/T_c = 0.4$ the seed loop travels azimuthally and undergoes the Kelvin-wave instability, when the superflow is oriented along the vortex [8]. Here $q < 1$ so that Kelvin wave oscillations are only lightly damped and loop formation starts via reconnections. Thus a vortex network develops already at the injection site. The vortex-free superflow above the tangle stretches the loops with right orientation, while others shrink, and thus the tangle extends and travels in the axial direction. Through reconnections the properly oriented loops are gradually joined to lines which form a bundle almost parallel to the rotation axis $\hat{\Omega}$. The bundle precesses initially around the $\hat{\Omega}$ axis, but presumably more reconnections of remaining loops will continue adding lines to the bundle and thereby reducing the superflow around the bundle, until the equilibrium number of rectilinear vortex lines is reached. The complete calculation is so far too time consuming.

Discussion:—Both the results from the numerical simulations in Fig. 1 and from the measurements in Fig. 2 support the conclusion from Eq. (1) that the transition to turbulence is determined by the parameter $q = \alpha/(1 - \alpha')$: There exists a critical value $q_c \approx 1$ which separates the mutual-friction-dominated regime at $q > q_c$ from the inertia-dominated turbulent regime at $q < q_c$. With $q > q_c$, the vortex-loop expansion is a regular stable process even in high-velocity superflow with $Re_s \gg 1$, as has been verified in many previous measurements. With $q < q_c$, a multiplication process is switched on, the vortex lines create loops, become entangled, and reconnect forming new loops. Could q_c be a fundamental universal number which, when $Re_s \gg 1$, places the upper bound to superfluid turbulence?

Why has such a transition, driven by an intrinsic pa-

rameter, not been observed previously in superfluid ^4He ? A number of reasons can be listed: (i) In ^3He the viscosity of the normal fraction is four orders of magnitude higher. Thus there is no ambiguity about the state of the normal component, unlike in the case of ^4He . (ii) The vortex-core radius in $^3\text{He-B}$ exceeds by two orders of magnitude that of ^4He , where it is only of atomic size. Therefore vortex pinning and remanence at solid walls can often be neglected in $^3\text{He-B}$ and metastable states with rapid superflow become possible. (iii) The most important difference lies in the value of mutual friction. In ^4He the dissipative part α is small and influences vortex motion relatively little. Only within a narrow temperature interval $\Delta T/T_\lambda \sim 2 \cdot 10^{-3}$ from T_λ one finds $q > 1$ and expects different behavior. No conclusive measurements exist from so close to T_λ .

In the helium superfluids, the transition at $q_c \approx 1$ lies very close to T_λ in ^4He , in the middle of the experimentally accessible temperature range in $^3\text{He-B}$, and below that at extremely low temperatures in $^3\text{He-A}$. This prediction is consistent with present experimental information. Here we found that turbulence is unstable even at high Re_s , if $q > q_c$. Perhaps in other multi-component hydrodynamic systems, superfluid or viscous, the stability of turbulence might also be governed by an intrinsic parameter, in addition to the Reynolds number.

-
- [1] Vinen, W.F. & Niemela, J.J. Quantum turbulence. *J. Low Temp. Phys.* **128**, 167 (2002).
 - [2] Ruutu, V.M.H. *et al.* Intrinsic and extrinsic mechanisms of vortex formation in superfluid $^3\text{He-B}$. *J. Low Temp. Phys.* **107**, 93 (1997). *Europhys. Lett.* **31**, 449 (1995).
 - [3] Ruutu, V.M.H. *et al.* Vortex formation in neutron-irradiated superfluid ^3He as an analogue of cosmological defect formation. *Nature* **382**, 334 (1996).
 - [4] Blaauwgeers, R. *et al.* Shear flow and Kelvin-Helmholtz instability in superfluids. *Phys. Rev. Lett.* **89**, 155301 (2002). *Physica B* in print (2003).
 - [5] Fisher, S.N. *et al.* Generation and detection of quantum turbulence in superfluid $^3\text{He-B}$. *Phys. Rev. Lett.* **86**, 244 (2001).
 - [6] See *eg.* text book by McComb, W.D. *The Physics of fluid turbulence* (Clarendon Press, Oxford, 1990).
 - [7] Sonin, E.B. Vortex oscillations and hydrodynamics of rotating superfluids. *Rev. Mod. Phys.* **59**, 87 (1987).
 - [8] Barenghi, C.F. *et al.* Thermal excitation of waves on quantized vortices. *Phys. Fluids* **28**, 498 (1985).
 - [9] Kopnin, N.B. *Theory of nonequilibrium superconductivity* (Clarendon Press, Oxford, 2001).
 - [10] Bevan, T.D.C. *et al.* Vortex mutual friction in superfluid ^3He . *J. Low Temp. Phys.* **109**, 423 (1997).
 - [11] Skrbek, L. *et al.* Vortex flow in rotating superfluid $^3\text{He-B}$. *Physica B* in print (2003). See also Fig. 19 and its explanation in Ref. [2].
 - [12] Schwarz, K.W. Three-dimensional vortex dynamics in superfluid ^4He : Homogeneous superfluid turbulence. *Phys. Rev. B* **38**, 2398 (1988). Tsubota, M. *et al.* Dynamics of vortex tangle without mutual friction in superfluid ^4He . *Phys. Rev. B* **62**, 11751 (2000).

- [13] Tsubota, M. *et al.* Rotating superfluid turbulence. *Preprint* cond-mat/0301412.

This work was supported in part by the following EU and ESF programmes: EU-IHP ULTI-3, ESF-COSLAB, ESF-VORTEX. NK and GV are grateful to the Russian Foundation for Basic Research; LS thanks for the grant GACR (202/02/0251). We thank W.F. Vinen for valuable discussion.